Supplementary Material

Two-dimensional Porous Silicon Nanosheets as Anode Materials for High Performance Lithium-ion Batteries

Jingjing Tang[a,d,1] , Qifang Yin[a,1] , Qian Wang[a], Qianqian Li[b], Hongtao Wang[c], Zhenglong Xu[a], Haimin Yao[a,*], Juan Yang[d], Xiangyang Zhou[d], Jang-Kyo Kim[e], Limin Zhou[a,*]

[a] Department of Mechanical and Engineering, The Hong Kong Polytechnic University, Hong Kong, China

[b] Materials Genome Institute, Shanghai University, Shanghai, China

[c] Institute of Applied Mechanics, Zhejiang University, Hangzhou, China

[d] School of Metallurgy and Environment, Central South University, Changsha, China

[e] Department of Mechanical and Aerospace Engineering, Hong Kong University of Science and Technology, Clear Water Bay, Hong Kong, China

E-mail address: mmhyao@polyu.edu.hk (H. Yao), li.min.zhou@polyu.edu.hk (L. Zhou).

[*] Corresponding authors.

E-mail address: mmhyao@polyu.edu.hk (H. Yao), li.min.zhou@polyu.edu.hk (L. Zhou).

[1] These two authors contributed equally to this work.

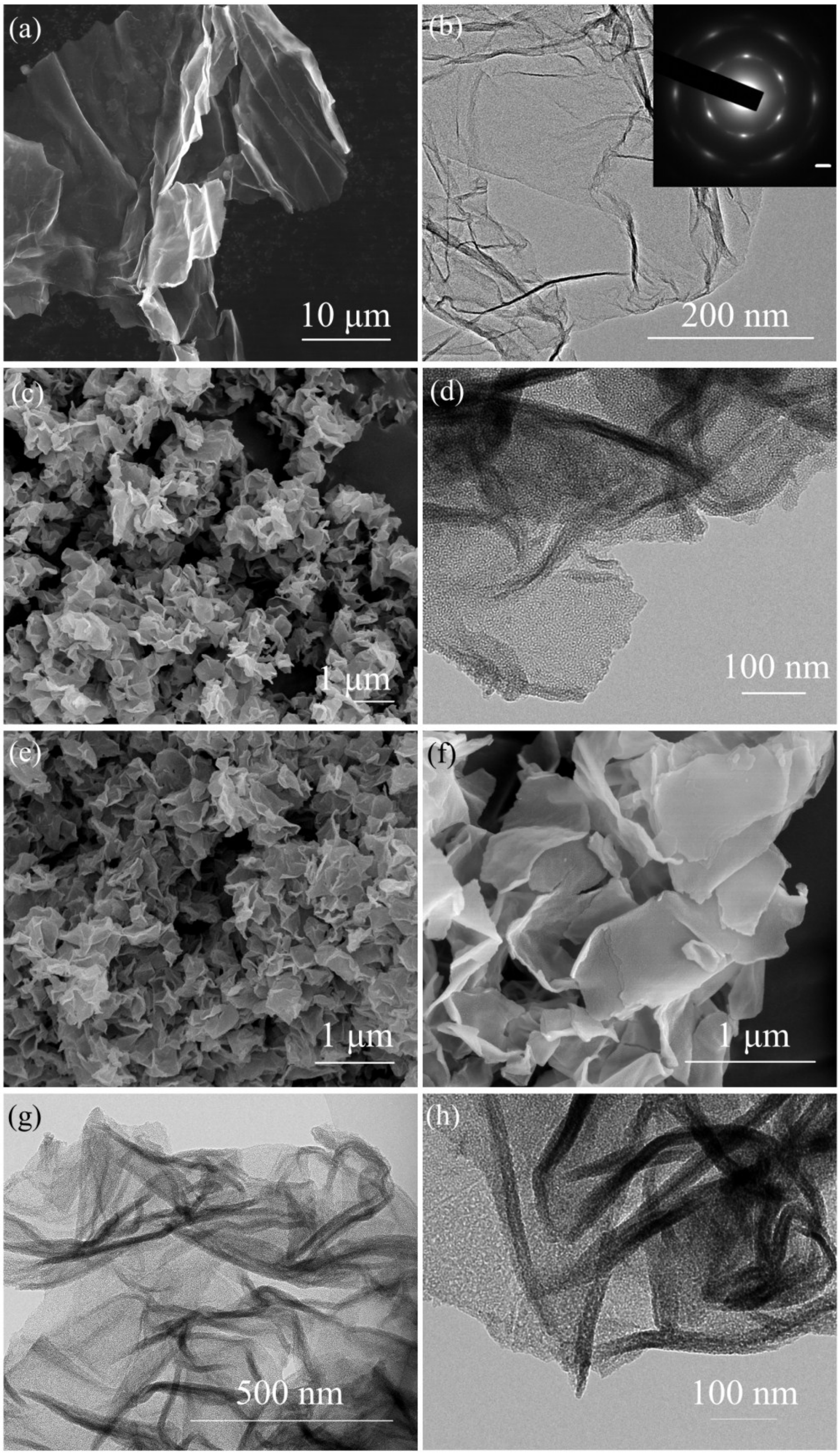

Fig. S1. (a) SEM and (b) TEM images of GO nanosheets; the inset of (b) is the SAED image of GO; (c) SEM and (d) TEM images of GO/SiO_2; (e, f) SEM and (g, h) TEM images of m-SiO_2.

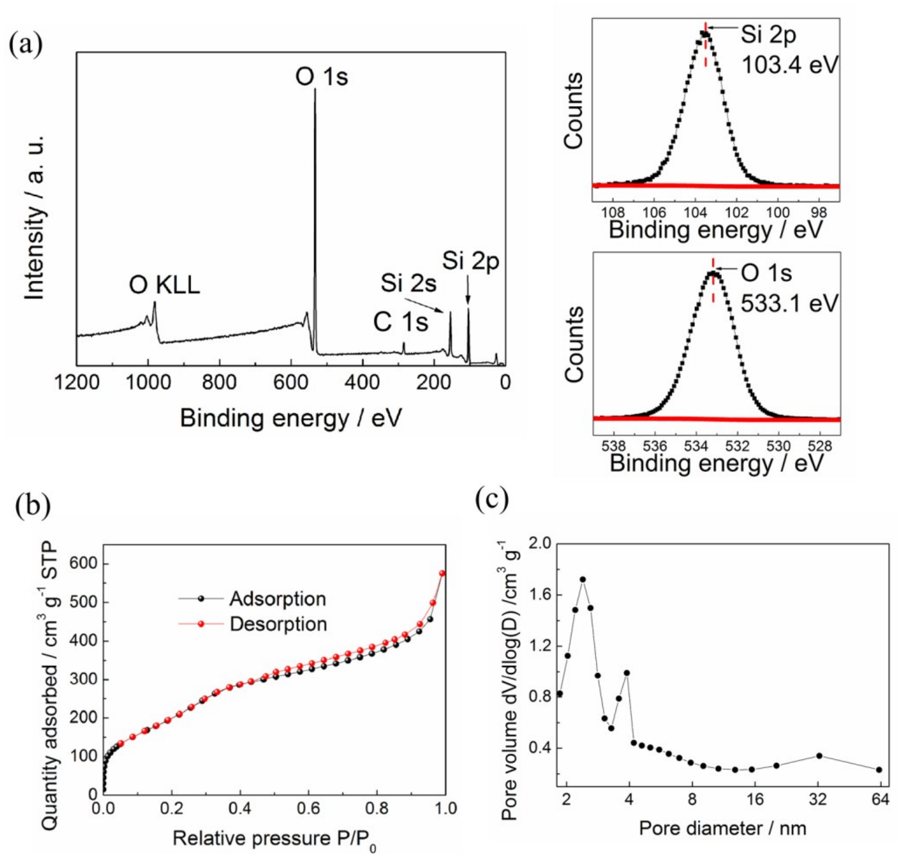

Fig. S2. (a) XPS spectrum, and Si 2p and O 1s XPS spectra of m-SiO_2; (b) N_2 sorption isotherm and (c) pore-size distribution of m-SiO_2.

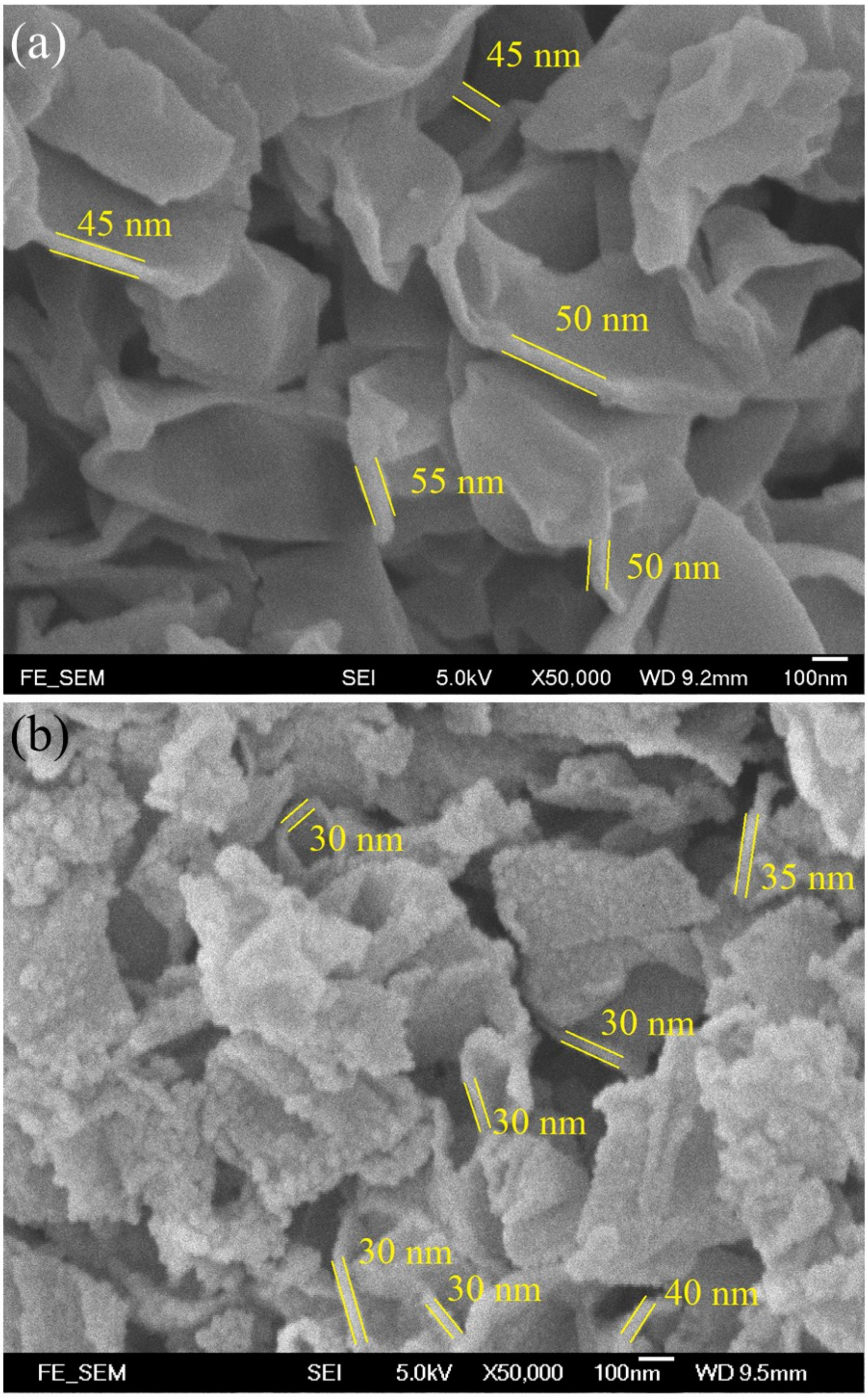

Fig. S3. SEM images of (a) m-SiO_2 and (b) Si-NSs.

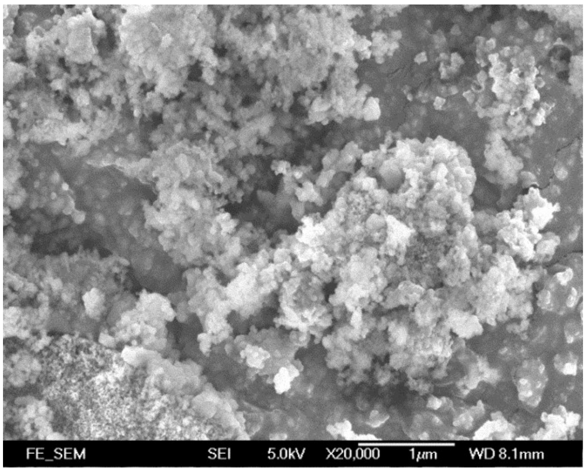

Fig. S4. SEM image of Si-W/O-NaCl obtained via thermic reduction of m-SiO_2 without addition of NaCl.

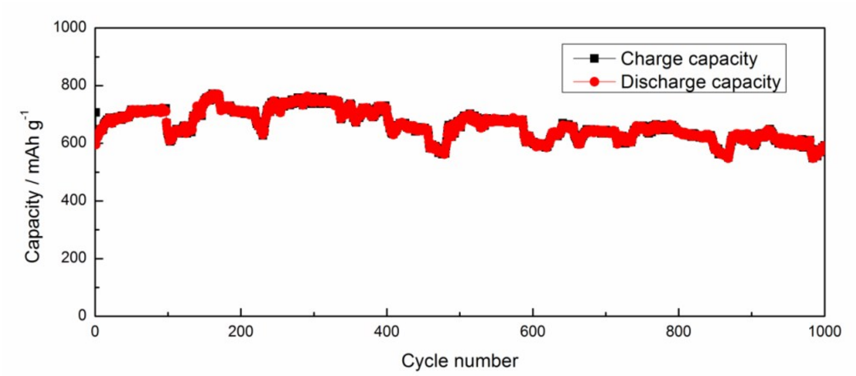

Fig. S5. Cycling performance of the tested Si-NSs anode after it is let stand for 10 days. The initial discharge capacity is 595 mAh g^{-1} and the capacity is still above 590 mAh g^{-1} even after 1000 more cycles.

Table S1. Comparison of electrochemical performance of reported bare nano-Si and Si-based nanocomposites.

Materials	**Electrochemical performances**	**References**
Commercial nano-Si particles	~2700 mAh g^{-1}/0.1C	This study
Si nanowires	~1000 mAh g^{-1}/0.95 C	S1
Si nanotubes	~500 mAh g^{-1}/1C ~250 mAh g^{-1}/2C	S2
Si nanowires@G sheaths@rGO	~1700 mAh g^{-1}/0.2C ~500 mAh g^{-1}/2C	S3
Si nanosheets	~1300 mAh g^{-1}/0.2C	S4
Si@C@G	~800 mAh g^{-1}/0.02C ~400 mAh g^{-1}/0.12C	S5
Granadilla-like Si@C	~650 mAh g^{-1}/0.48C	S6
Electrospun Si@C nanofibers	~1200 mAh g^{-1}/0.05C ~750 mAh g^{-1}/0.48C	S7
Self-supporting Si@G	~1500 mAh g^{-1}/0.48C	S8
Si/porous carbon	~1500 mAh g^{-1}/0.95C	S9
Si@TiO_{2-x}@C	~1000 mAh g^{-1}/1C	S10
Yolk-shell Si@C	~1000 mAh g^{-1}/0.1C	S11
Si@Void@C nanotubes	~1000 mAh g^{-1}/1C	S12
Si-NSs	~2500 mAh g^{-1}/0.1C ~1000 mAh g^{-1}/2C	This study

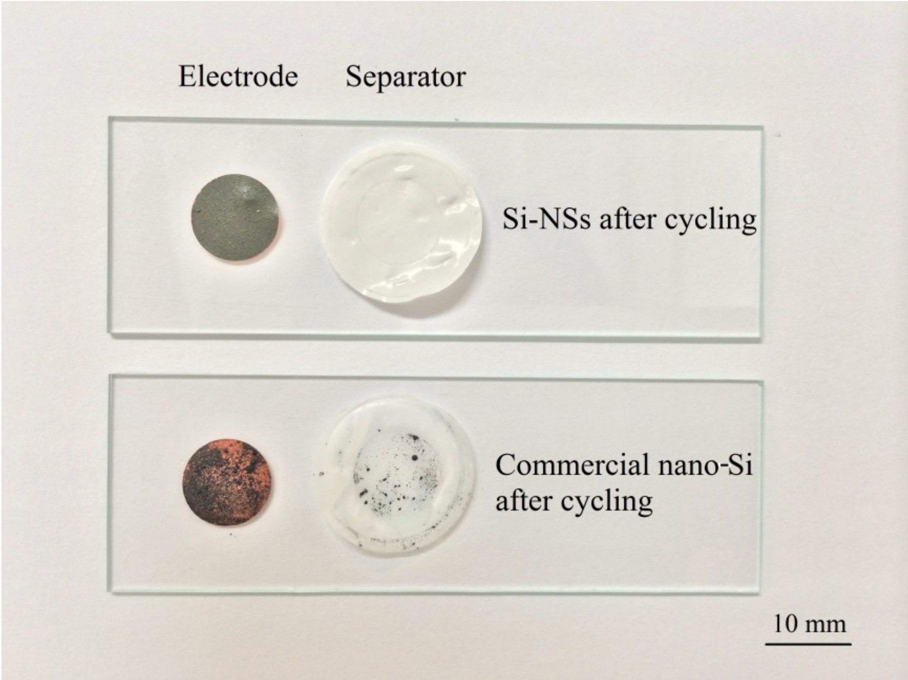

Fig. S5. Images of Si-NSs and commercial nano Si electrodes after 100 cycles at 0.2 C.

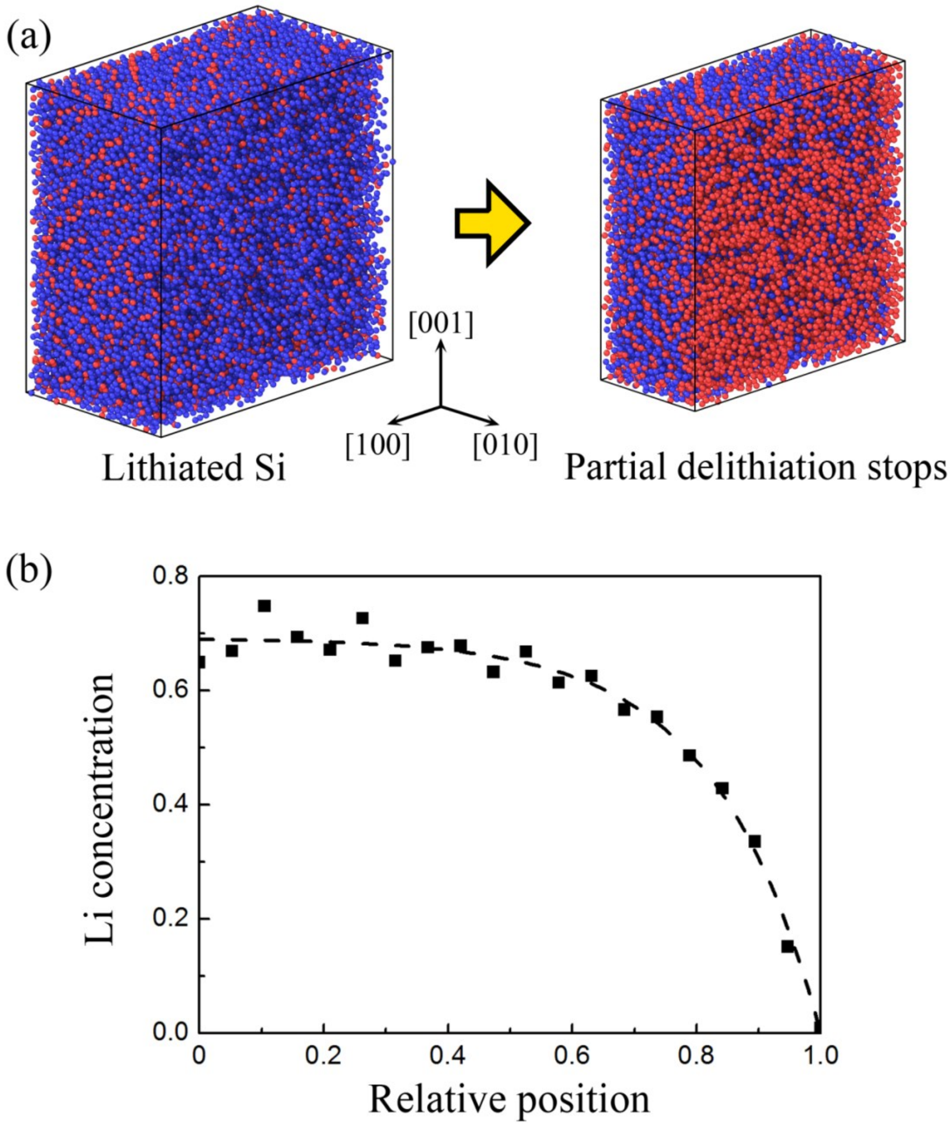

Fig. S6. The illustration of the partial delithiation mode. Delithiation is achieved by randomly removing Li atoms from the (010) surface of the lithiated Si model, which induces a Li concentration gradient. During the delithiation process, Li atoms far from the surface would be driven by the concentration gradient through the cell to the surface. It stops once the number fraction of Li on this surface reaches zero. (a) The illustration of the anode when delithiation starts and stops. Red and blue spheres are for Si and Li atoms, respectively. Before delithiation starts, the atom number ratio of Li and Si is 3.75:1. (b) The profile of Li concentration along [010] direction right when partial delithiation stops. About 62% of Li atoms are removed before delithiation stops, corresponding to an atom number ratio of Li and Si of 1.42:1. The remaining Li atoms in the Si anode are analogous to the capacity loss caused by various facts such as the formation of SEI. The dashed line is the exponential fitting of the squares.

References

[S1] M. Ge, J. Rong, X. Fang, C. Zhou, Porous doped silicon nanowires for lithium ion battery anode with long cycle life, Nano Lett. 12 (2012) 2318-2323.

[S2] Z. Wen, G. Lu, S. Mao, H. Kim, S. Cui, K. Yu, X. Huang, P.T. Hurley, O. Mao, J. Chen, Silicon nanotube anode for lithium-ion batteries, Electrochem. Commun. 29 (2013) 67-70.

[S3] B. Wang, X. Li, X. Zhang, B. Luo, M. Jin, M. Liang, S.A. Dayeh, S. Picraux, L. Zhi, Adaptable silicon–carbon nanocables sandwiched between reduced graphene oxide sheets as lithium ion battery anodes, ACS nano 7 (2013) 1437-1445.

[S4] J. Ryu, D. Hong, S. Choi, S. Park, Synthesis of ultrathin Si nanosheets from natural clays for lithium-ion battery anodes, ACS nano 10 (2016) 2843-2851.

[S5] J. Wang, D.-H. Liu, Y.-Y. Wang, B.-H. Hou, J.-P. Zhang, R.-S. Wang, X.-L. Wu, Dual-carbon enhanced silicon-based composite as superior anode material for lithium ion batteries, J Power Sources 307 (2016) 738-745.

[S6] L. Zhang, R. Rajagopalan, H. Guo, X. Hu, S. Dou, H. Liu, A Green and Facile Way to

Prepare Granadilla‐Like Silicon‐Based Anode Materials for Li‐Ion Batteries, Adv. Funct. Mater. 26 (2016) 440-446.

[S7] J. Wu, X. Qin, C. Miao, Y.-B. He, G. Liang, D. Zhou, M. Liu, C. Han, B. Li, F. Kang, A honeycomb-cobweb inspired hierarchical core–shell structure design for electrospun silicon/carbon fibers as lithium-ion battery anodes, Carbon 98 (2016) 582-591.

[S8] M. Zhou, X. Li, B. Wang, Y. Zhang, J. Ning, Z. Xiao, X. Zhang, Y. Chang, L. Zhi, High-performance silicon battery anodes enabled by engineering graphene assemblies, Nano Lett. 15 (2015) 6222-6228.

[S9] D.S. Jung, T.H. Hwang, S.B. Park, J.W. Choi, Spray drying method for large-scale and high-performance silicon negative electrodes in Li-ion batteries, Nano Lett. 13 (2013) 2092-2097.

[S10] G. Jeong, J.-G. Kim, M.-S. Park, M. Seo, S.M. Hwang, Y.-U. Kim, Y.-J. Kim, J.H. Kim, S.X. Dou, Core–shell structured silicon nanoparticles@ TiO2–x/carbon mesoporous microfiber composite as a safe and high-performance lithium-ion battery anode, Acs Nano 8 (2014) 2977-2985.

[S11] J. Yang, Y.-X. Wang, S.-L. Chou, R. Zhang, Y. Xu, J. Fan, W.-x. Zhang, H.K. Liu, D. Zhao, S.X. Dou, Yolk-shell silicon-mesoporous carbon anode with compact solid electrolyte interphase film for superior lithium-ion batteries, Nano Energy 18 (2015) 133-142.

[S12] B. Wang, X. Li, X. Zhang, B. Luo, Y. Zhang, L. Zhi, Contact‐engineered and void‐involved silicon/carbon nanohybrids as lithium‐ion‐battery anodes, Adv. Mater. 25 (2013) 3560-3565.

[S13] M. Gu, Y. Li, X.L. Li, S.Y. Hu, X.W. Zhang, W. Xu, S. Thevuthasan, D.R. Baer, J.G. Zhang, J. Liu, C.M. Wang, In Situ TEM Study of Lithiation Behavior of Silicon Nanoparticles Attached to and Embedded in a Carbon Matrix, Acs Nano 6 (2012) 8439-8447.

[S14] X.H. Liu, S. Huang, S.T. Picraux, J. Li, T. Zhu, J.Y. Huang, Reversible Nanopore Formation in Ge Nanowires during Lithiation-Delithiation Cycling: An In Situ Transmission Electron Microscopy Study, Nano Lett. 11 (2011) 3991-3997.

[S15] J.W. Choi, J. McDonough, S. Jeong, J.S. Yoo, C.K. Chan, Y. Cui, Stepwise Nanopore Evolution in One-Dimensional Nanostructures, Nano Lett. 10 (2010) 1409-1413.